

Design of a memristive chaotic map and its adaptive regulation

Ya Wang(王亚), Xin-Lin Song(宋欣林), and Fei-Fei Yang(杨飞飞)
Citatio: Chin. Phys. B, 2025, 34 (**9**): 090504. DOI: 10.1088/1674-1056/adea5c
http://cpb.iphy.ac.cn; http://iopscience.iop.org/cpb

What follows is a list of articles you may be interested in

Chaos of cavity optomechanical system with Coulomb coupling

Yingjia Yang(杨应佳), Liwei Liu(刘利伟), Lianchun Yu(俞连春), Weizheng Kong(孔伟正), Haiyan Jiao(焦海燕), Xiaoyan Deng(邓小燕), and Xiaoyong Li(李小勇)
Chin. Phys. B, 2025, 34 (**8**): 080503. DOI: 10.1088/1674-1056/add509

Generation of multitype, multicavity chaotic attractors via impulse-function-based state variable extension

Xiaoyu Hu(胡晓宇), Siteng Wang(王思腾), Panpan Wu(邬盼盼), Hongbo Cao(曹红博), Tianwei Yang(杨天纬), and Zhongshuo Dong(董忠硕)
Chin. Phys. B, 2025, 34 (**8**): 080502. DOI: 10.1088/1674-1056/add249

Extremely hidden multi-stability in a class of two-dimensional maps with a cosine memristor

Li-Ping Zhang(张丽萍), Yang Liu(刘洋), Zhou-Chao Wei(魏周超), Hai-Bo Jiang(姜海波), Wei-Peng Lyu(吕伟鹏), and Qin-Sheng Bi(毕勤胜)
Chin. Phys. B, 2022, 31 (**10**): 100503. DOI: 10.1088/1674-1056/ac7294

Cascade discrete memristive maps for enhancing chaos

Fang Yuan(袁方), Cheng-Jun Bai(柏承君), and Yu-Xia Li(李玉霞)
Chin. Phys. B, 2021, 30 (**12**): 120514. DOI: 10.1088/1674-1056/ac20c7

A memristive map with coexisting chaos and hyperchaos

Sixiao Kong(孔思晓), Chunbiao Li(李春彪), Shaobo He(贺少波), Serdar Çiçek, and Qiang Lai(赖强)
Chin. Phys. B, 2021, 30 (**11**): 110502. DOI: 10.1088/1674-1056/abf4fb

---

Design of a memristive chaotic map and its adaptive regulation

Ya Wang(王亚)[1], Xin-Lin Song(宋欣林)[2,†], and Fei-Fei Yang(杨飞飞)[3]

[1] *School of Cyber Security, Gansu University of Political Science and Law, Lanzhou* 730070, *China*
[2] *College of Science, Xi'an University of Science and Technology, Xi'an* 710054, *China*
[3] *College of Artificial Intelligence and Computer Science, Xi'an University of Science and Technology, Xi'an* 710054, *China*

(Received 18 May 2025; revised manuscript received 18 June 2025; accepted manuscript online 1 July 2025)

The analysis of structure and dynamics in chaotic systems has long been a significant research direction in nonlinear science. Constructing a reliable chaotic system with rich dynamical characteristics is essential for secure communication applications. Existing memristor-based chaotic maps are typically obtained by incorporating discrete mathematical models of memristors into basic chaotic maps. In this study, a simple memristive nonlinear circuit is first designed, from which a memristive oscillator is derived. Subsequently, a memristive map is developed from this oscillator through a linear transformation of the variables. The reliability of the new map is validated through nonlinear dynamic analysis. The results demonstrate that the map exhibits complex nonlinear dynamics under different parameter settings. This finding is beneficial for the construction of memristor maps and the development of image encryption algorithms.

Keywords: memristive map, dynamic performance, adaptive regulation of energy

PACS: 05.45.–a

DOI: 10.1088/1674-1056/adea5c **CSTR:** 32038.14.CPB.adea5c

1. Introduction

Memristors are electrical elements with rich physical characteristics and unique functionalities. They are often incorporated into nonlinear circuits to enhance circuit functionality and controllability. Memristors are employed to enhance the dynamics of chaotic systems. In fact, memristors have been extensively studied in neuroscience and nonlinear science. Specifically, it is crucial to explore the structure of memristor systems and analyze their dynamical characteristics for applications of memristor-based chaotic systems in secure communication and image encryption.[1,2]

Based on the nonlinear characteristics of memristors, numerous memristive nonlinear circuits and chaotic systems have been developed. Examples include discrete-time memristor circuits,[3,4] magnetic flux-controlled memristor (MFCM) circuits,[5–9] charge-controlled memristor (CCM) circuits,[10] dual memristor circuits,[11,12] MFCM chaotic systems,[13–15] CCM chaotic systems,[16] and other memristive chaotic systems.[17–22] In addition, these memristive chaotic systems have been applied in image encryption algorithms.[23–27] Recently, various memristor neuron models have been proposed, including CCM neurons,[28] MFCM neurons,[29] dual memristive neurons,[30,31] memristive membrane neurons[32,33], and other memristive neuron models[34–39] and networks.[40,41]

The aforementioned studies primarily focus on memristor oscillator models. Memristive maps constitute another interesting research area. Several memristive maps have been investigated, such as memristive chaotic maps,[42–44] memristive hyperchaotic maps[45–47], and memristive map neurons.[48–51] These maps are usually designed based on existing mapping models and discrete memristor mathematical models, rather than being derived from physical electronic circuits. For practical engineering applications, digital implementations of memristive maps can be realized using digital signal processing (DSP) hardware.[52–54] Accordingly, researchers have developed memristive maps[55,56] and memristive map neurons[57,58] based on nonlinear memristive circuits. However, these circuit-based memristive maps typically do not account for external input signals. Therefore, to explore the effect of input signals on the dynamics of memristive maps, this paper constructs a memristive chaotic map based on a memristive nonlinear circuit. The key contributions of this study are summarized as follows: (1) An external input signal is incorporated into a memristive nonlinear circuit. (2) A memristive map is developed from a memristive oscillator generated by the memristive circuit. (3) An adaptive parameter growth method is proposed.

The article is organized as follows: the construction of the memristive map is described in Section 2. Nonlinear dynamics of the memristive map are analyzed in Section 3. Finally, the main conclusions of this study are summarized in Section 4.

2. Model of 3D memristive map

Incorporating a memristor into a nonlinear circuit can enhance the dynamic performance of the circuit. In this work, a memristive circuit is built based on a magnetic flux-controlled

†Corresponding author. E-mail: xinlinsong@xust.edu.cn

© 2025 Chinese Physical Society and IOP Publishing Ltd. All rights, including for text and data mining, AI training, and similar technologies, are reserved.

memristor, a capacitor, a nonlinear resistor, an inductor, and an ordinary resistor. The structure of the memristive circuit is shown in Fig. 1.

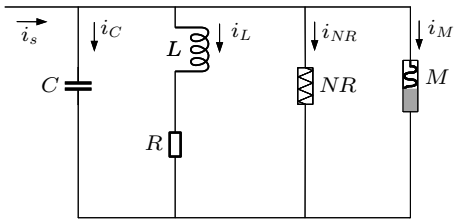


Fig. 1. A nonlinear circuit with a single memristive channel.

The current i_{NR} in Fig. 1 is expressed as

$$i_{NR} = -\frac{r}{\rho}\left(V - \frac{V^2}{V_0}\right), \tag{1}$$

where $(\rho,\ r)$ denotes the mean resistance and gain of the nonlinear resistor, and $(V,\ V_0)$ denotes the voltage across the nonlinear resistor and the cut-off voltage. A magnetic flux-controlled memristor is described by

$$\begin{cases} i_M = \varphi V_M, \\ \dfrac{\mathrm{d}\varphi}{\mathrm{d}t} = a\varphi + bV_M, \end{cases} \tag{2}$$

where $(a,\ b)$ are parameters related to the memristor materials. Applying Kirchhoff's current and voltage laws, the circuit equations can be derived as

$$\begin{cases} C\dfrac{\mathrm{d}V}{\mathrm{d}t} = i_s - i_L - i_{NR} - i_M, \\ L\dfrac{\mathrm{d}i_L}{\mathrm{d}t} = V - Ri_L, \\ \dfrac{\mathrm{d}\varphi}{\mathrm{d}t} = a\varphi + bV. \end{cases} \tag{3}$$

The variables in Eq. (3) are defined as

$$x = \frac{V}{V_0},\quad y = \frac{\rho i_L}{V_0},\quad z = \frac{\varphi}{\rho C V_0},\quad \tau = \frac{t}{\rho C}. \tag{4}$$

Thus, the model in Eq. (3) can be rewritten as

$$\begin{cases} \dfrac{\mathrm{d}x}{\mathrm{d}\tau} = r(x - x^2) - y - \alpha z x + u_s, \\ \dfrac{\mathrm{d}y}{\mathrm{d}\tau} = c\,(x - \beta y), \\ \dfrac{\mathrm{d}z}{\mathrm{d}\tau} = dz + bx, \end{cases} \tag{5}$$

with parameters defined as

$$\alpha = \rho^2 C V_0,\ \ \beta = \frac{R}{\rho},\ \ c = \frac{\rho^2 C}{L},\ \ d = a\rho C,\ \ u_s = \frac{\rho}{V_0} i_s. \tag{6}$$

In Fig. 1, the physical energy of the storage elements and the dimensionless energy are calculated by

$$W = \frac{1}{2}CV^2 + \frac{1}{2}Li^2 + \frac{1}{2}\varphi i_M,$$

$$H = \frac{W}{CV_0^2} = \frac{1}{2}x^2 + \frac{1}{2c}y^2 + \frac{1}{2}\alpha z^2 x. \tag{7}$$

The oscillator model in Eq. (5) can equivalently be expressed in vector form as

$$\begin{aligned} \begin{pmatrix} \mathrm{d}x/\mathrm{d}\tau \\ \mathrm{d}y/\mathrm{d}\tau \\ \mathrm{d}z/\mathrm{d}\tau \end{pmatrix} &= \begin{pmatrix} r(x-x^2) - y - \alpha z x + u_s \\ c(x - \beta y) \\ dz + bx \end{pmatrix} = \boldsymbol{F}_c + \boldsymbol{F}_d \\ &= \begin{pmatrix} -y - \alpha b z x \\ cx + 0.5c\alpha z^2 \\ bx + 0.5\alpha b z^2 \end{pmatrix} \\ &\quad + \begin{pmatrix} r(x-x^2) + \alpha b z x - \alpha z x + u_s \\ -c\beta y - 0.5c\alpha z^2 \\ dz - 0.5\alpha b z^2 \end{pmatrix} \\ &= \begin{pmatrix} 0 & -c & -b \\ c & 0 & 0 \\ b & 0 & 0 \end{pmatrix} \begin{pmatrix} x + 0.5\alpha z^2 \\ y/c \\ \alpha z x \end{pmatrix} \\ &\quad + \begin{pmatrix} A_1 & 0 & 0 \\ 0 & A_2 & 0 \\ 0 & 0 & A_3 \end{pmatrix} \begin{pmatrix} x + 0.5\alpha z^2 \\ y/c \\ \alpha z x \end{pmatrix}, \end{aligned}$$

$$\begin{aligned} A_1 &= \frac{r(x-x^2) + \alpha b z x - \alpha z x + u_s}{x + 0.5\alpha z^2}, \\ A_2 &= \frac{-c\beta y - 0.5c\alpha z^2}{y/c}, \\ A_3 &= \frac{dz - 0.5\alpha b z^2}{\alpha z x}. \end{aligned} \tag{8}$$

The energy defined in Eq. (7) satisfies the following conditions:

$$\nabla H^{\mathrm{T}} f_c(x,y,z) = 0,\quad \nabla H^{\mathrm{T}} f_d(x,y,z) = \dot{H} = \frac{\mathrm{d}H}{\mathrm{d}t}. \tag{9}$$

Specifically,

$$\begin{aligned} \nabla H^{\mathrm{T}} F_c &= (-y - \alpha b z x)\frac{\partial H}{\partial x} + (cx + 0.5c\alpha z^2)\frac{\partial H}{\partial y} \\ &\quad + (bx + 0.5\alpha b z^2)\frac{\partial H}{\partial z} = 0. \end{aligned} \tag{10}$$

The memristive oscillator in Eq. (5) can be converted into a map model using the Euler difference algorithm. Furthermore, the variables in Eq. (5) are linearly transformed according to Eq. (11):

$$u_n = \frac{r\Delta\tau}{1 + r\Delta\tau} x_n,\quad v_n = \frac{r\Delta\tau}{1 + r\Delta\tau} y_n,\quad w_n = \frac{r\Delta\tau}{1 + r\Delta\tau} z_n, \tag{11}$$

where $\Delta\tau$ is the time step for the numerical approximation of Eq. (5). As a result, a memristive map is obtained as follows:

$$\begin{cases} u_{n+1} = \lambda(u_n - u_n^2) - \delta v_n - \chi w_n u_n + \gamma, \\ v_{n+1} = k(u_n - e v_n), \\ w_{n+1} = \sigma u_n + f w_n. \end{cases} \tag{12}$$

The parameters in Eq. (11) are defined by

$$\begin{cases} \gamma = \dfrac{r(\Delta\tau)^2}{1 + r\Delta\tau} u_s,\quad \chi = \dfrac{\alpha(1 + r\Delta\tau)}{r}, \\ \delta = \Delta\tau,\quad \lambda = 1 + r\Delta\tau, \\ \sigma = d\Delta\tau,\quad k = c\Delta\tau, \\ e = -\dfrac{1}{c\Delta\tau} + \beta,\quad f = b\Delta\tau + 1. \end{cases} \tag{13}$$

Similarly, the energy function of the memristive map in Eq. (11) is given by

$$H_n = \frac{1}{2}u_n^2 + \frac{1}{2k}v_n^2 + \frac{1}{2}\chi u_n w_n^2. \tag{14}$$

3. Dynamic analysis of a derived chaotic map

In this section, the nonlinear dynamics of the chaotic map in Eq. (12) are explored using nonlinear analysis methods. Initially, the parameters in Eq. (12) are set as $\lambda = 3.74$, $\delta = \chi = \gamma = e = 0.1$, $\sigma = 3$, and $f = 0.4$, with the initial value $(0.1, 0.2, 0.3)$. The influence of parameter κ on the map dynamics is analyzed, as shown in Fig. 2.

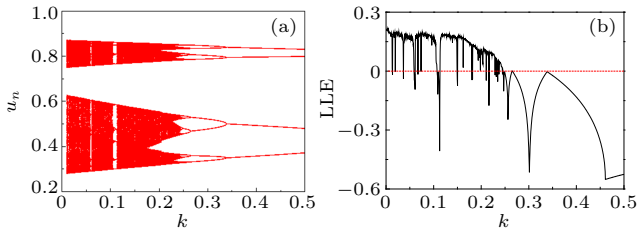


Fig. 2. Dynamic characteristics of the chaotic map in Eq. (12) under varying parameters. (a) Bifurcation diagram for $k \in [0, 0.5]$. (b) Largest Lyapunov exponent (LLE) for $k \in [0, 0.5]$.

The bifurcation diagram in Fig. 2(a) shows that periodic and chaotic modes in the memristive map can be obtained by adjusting parameter κ, while Fig. 2(b) indicates that the periodic state has an LLE less than zero, and the chaotic state has a positive LLE. With the same parameters and initial values, the phase portraits of the memristive map are plotted for different values of k, as shown in Fig. 3.

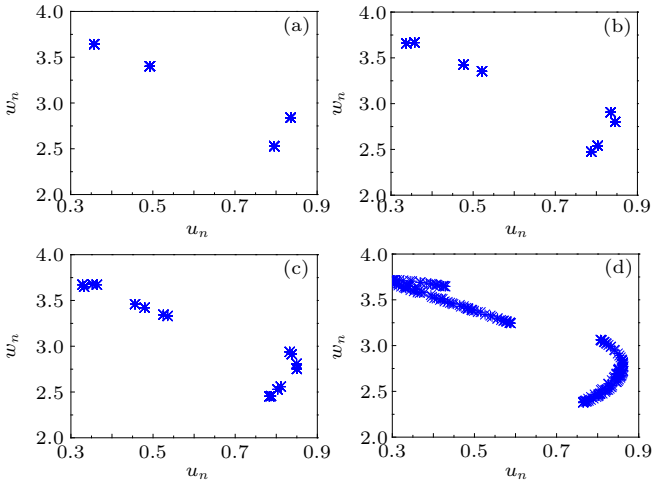


Fig. 3. Phase diagrams for different k. (a) $k = 0.4$, periodic; (b) $k = 0.3$, periodic; (c) $k = 0.25$, periodic; (d) $k = 0.1$, chaotic.

The results in Fig. 3 demonstrate that different phase portraits corresponding to periodic and chaotic states can be formed by varying k. Figure 4 shows the energy evolution for these states.

Figure 4 shows that the periodic state exhibits a higher average energy, while the chaotic pattern has a lower average energy. During the transition from the periodic to the chaotic state, the average energy decreases continuously.

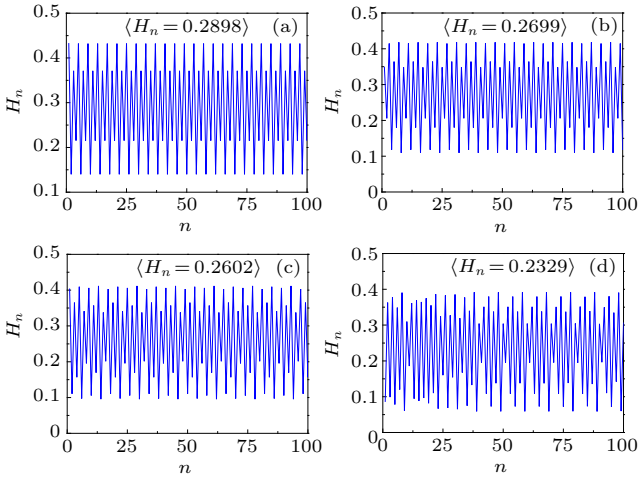


Fig. 4. Energy evolution for different periodic and chaotic patterns. (a) $k = 0.4$; (b) $k = 0.3$; (c) $k = 0.25$; (d) $k = 0.1$. $\langle H_n \rangle$ denotes the average energy.

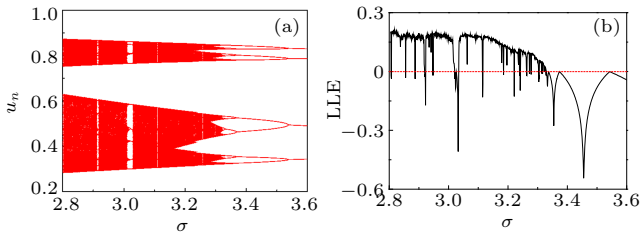


Fig. 5. Effect of parameter σ on the dynamics of the memristive map. (a) Bifurcation diagram for $\sigma \in [2.8, 3.6]$; (b) LLE for $\sigma \in [2.8, 3.6]$.

The influence of other parameters on the map dynamics is also explored. With $k = 0.1$, the bifurcation diagram and LLE for varying σ are shown in Fig. 5, demonstrating that setting different σ values produces rich dynamics, including chaotic and various periodic states. Similarly, the corresponding phase portraits are shown in Fig. 6.

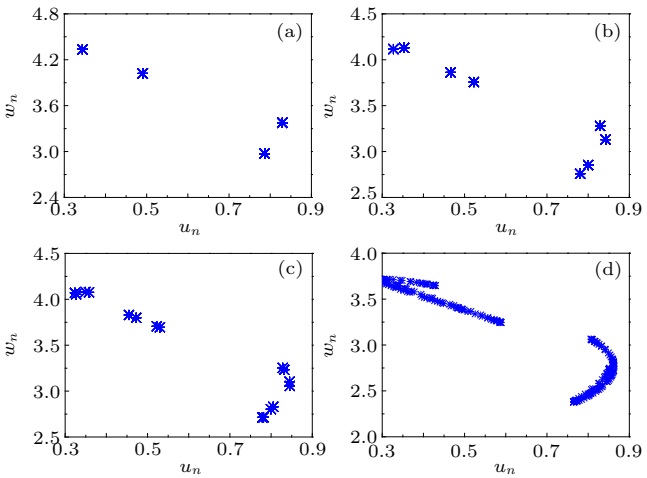


Fig. 6. Phase portraits for different values of σ. (a) $\sigma = 3.6$, periodic; (b) $\sigma = 3.4$, periodic; (c) $\sigma = 3.35$, periodic; (d) $\sigma = 3$, chaotic.

Different phase portraits can thus be generated by controlling σ. The effect of parameter γ is investigated next, with

$k = 0.1$, $\sigma = 2.9$, and other conditions unchanged. The results are shown in Fig. 7.

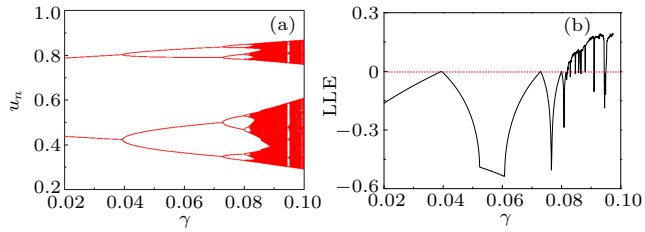


Fig. 7. Effect of parameter γ on map dynamics. (a) Bifurcation diagram for $\gamma \in [0.02, 0.1]$; (b) LLE for $\gamma \in [0.02, 0.1]$.

Similar to Figs. 2 and 5, the complex dynamics of the memristive map can be tuned by varying γ. The corresponding phase diagrams are shown in Fig. 8.

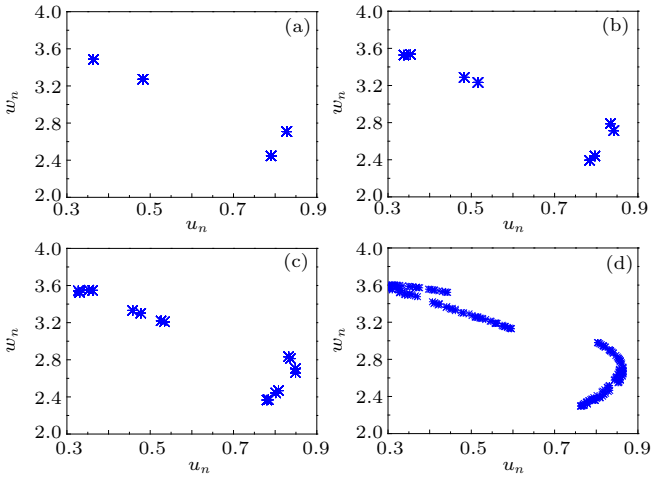


Fig. 8. Phase portraits for different γ. (a) $\gamma = 0.06$, periodic; (b) $\gamma = 0.075$, periodic; (c) $\gamma = 0.08$, periodic; (d) $\gamma = 0.097$, chaotic.

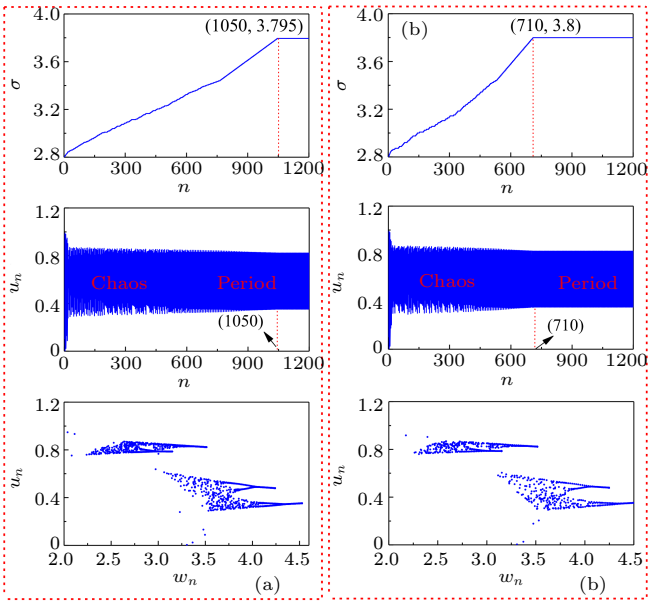


Fig. 9. Evolution of parameter σ, sequence of variable u_n, and phase diagrams. (a) $g = 0.005$; (b) $g = 0.008$.

To investigate adaptive regulation of energy on the dynamics, an adaptive growth method for σ is defined as

$$\sigma = \sigma_0 + g \cdot \theta(\varepsilon - H_n), \quad \theta(v) = 1, \quad v \geq 0;$$
$$\theta(v) = 0, \quad v < 0, \tag{15}$$

where σ_0 is the initial value of σ, g is the gain, and ε is the energy threshold. θ is the Heaviside function controlling σ growth. For $\sigma_0 = 2.8$, $k = 0.1$, $\varepsilon = 0.28$, and other conditions unchanged, the evolution of σ, u_n, and phase portraits for different g are shown in Fig. 9.

The results confirm that σ can be adaptively controlled using the method in Eqs. (14) and (15). With $g = 0.005$, σ stabilizes at 3.795 after 1050 iterations; increasing g to 0.008, σ stabilizes at 3.8 after 710 iterations. Hence, increasing the gain allows σ to reach stability more quickly. Other parameters can also be controlled adaptively using Eq. (15).

4. Conclusion

In this work, a 3D memristive map is developed from a 3D memristive oscillator generated by a nonlinear memristive circuit. Nonlinear dynamic analysis demonstrates that the memristive map exhibits complex dynamics by controlling the values of the parameters. In particular, different periodic and chaotic patterns can be generated by adjusting the parameters, with the periodic mode exhibiting a higher average energy, while the chaotic pattern has a lower one. During the evolution from the periodic state to the chaotic state, the average energy decreases continuously.

Furthermore, an adaptive growth method for the parameters based on the energy value is proposed to explore the adaptive characteristics of the memristive map. The results indicate that the parameters can be adaptively regulated using the proposed energy-based adaptive growth method. In addition, this memristive map can be further utilized and chaotically tuned through offset boosting and amplitude control to achieve coexistence of chaos and hyperchaos,[59–62] which is useful for chaotic image encryption.[1,2]

Acknowledgement

This study is supported by the Youth Innovation Team of Shaanxi Universities.

References

[1] Du Y, Long G, Jiang D, Chai X and Han J 2023 *Chin. Phys. B* **32** 114203
[2] Qiu D, Zhang B, Zhang T, Liu S and He P 2025 *Chin. Phys. B* **34** 040203
[3] Marco M D, Forti M, Pancioni L and Tesi A 2024 *Nonlinear Dyn.* **112** 13519
[4] Marco M D, Forti M, Pancioni L and Tesi A 2024 *Int. J. Bifurc. Chaos* **34** 2450001
[5] Li C, Yang Y, Du J and Chen Z 2021 *Eur. Phys. J. Spéc. Top.* **230** 1723
[6] Luo J, Tang W, Chen Y, Chen X and Zhou H 2023 *Results Phys.* **54** 107085
[7] Batas D and Fiedler H 2011 *IEEE Trans. Nanotechnol.* **10** 250
[8] Yang N, Xu C, Wu C, Jia R and Liu C 2019 *Nonlinear Dyn.* **97** 33

[9] Liu W, Wang F Q and Ma X K 2014 *Int. J. Numer. Model.: Electron. Netw., Devices Fields* **28** 335
[10] Si G, Diao L and Zhu J 2016 *Nonlinear Dyn.* **87** 2625
[11] Wu S, Rong X and Liu Z 2018 *Journal of System Simulation* **30** 3985
[12] Sun J, Yang J, Liu P and Wang Y 2023 *IEEE Trans. Comput.-Aided Des. Integr. Circuits Syst.* **42** 956
[13] Wang R, Li C, Kong S, Jiang Y and Lei T 2022 *Chaos, Solitons Fractals* **158** 111992
[14] Yan D, Jié M, Wang L and Duan S 2021 *Eur. Phys. J. Plus* **136** 1086
[15] Ramamoorthy R, Rajagopal K, Leutcho G D, Krejcar O, Namazi H and Hussain I 2022 *Chaos, Solitons Fractals* **156** 111834
[16] Sahin M E, Taskiran Z G C, Guler H and Hamamci S E 2020 *Circuits, Syst., Signal Process.* **39** 3320
[17] Gokyildirim A, Calgan H and Demirtas M 2023 *J. Vib. Control* **30** 1604
[18] Bao B C, Bao H, Wang N, Chen M and Xu Q 2017 *Chaos, Solitons Fractals* **94** 102
[19] Zhang L, Li Z and Peng Y 2024 *Chaos, Solitons Fractals* **185** 115109
[20] Dong C and Yang M 2024 *Fractal Fract.* **8** 266
[21] Yuan Y, Yu F, Tan B, Huang Y, Yao W, Cai S and Lin H 2025 *Chaos: Interdiscip. J. Nonlinear Sci.* **35** 013121
[22] Ahmed G 2024 *Eur. J. Pure Appl. Math.* **17** 835
[23] He S, Yang H, Li C and Shen X 2024 *Int. J. Bifurc. Chaos* **34** 2450138
[24] Zhang J, Liu E and Guo Y 2024 *J. Supercomput.* **80** 14694
[25] Ding P, Wang Z and Li K 2024 *Phys. Scr.* **99** 075252
[26] An X, Liu S, Xiong L, Zhang J and Li X 2024 *Expert Syst. Appl.* **243** 122899
[27] Kumar B S and Revathi R 2024 *IETE J. Res.* **70** 8160
[28] Yang F, Xu Y and Ma J 2023 *Chaos: Interdiscip. J. Nonlinear Sci.* **33** 023110
[29] Yang F, Han Z, Ren G, Guo Q and Ma J 2024 *Eur. Phys. J. Plus* **139** 534
[30] Yang F, Ren G and Tang J 2023 *Nonlinear Dyn.* **111** 21917
[31] Song X and Yang F 2025 *J. Theor. Biol.* **599** 112034
[32] Yang F, Song X and Yu Z 2024 *Chaos, Solitons Fractals* **188** 115496
[33] Guo Y, Wu F, Yang F and Ma J 2023 *Chaos: Interdiscip. J. Nonlinear Sci.* **33** 113106
[34] Babacan Y, Kaçar F and Gürkan K 2016 *Neurocomputing* **203** 86
[35] Chen X, Wang N, Wang K, Chen M, Parastesh F and Xu Q 2024 *Nonlinear Dyn.* **112** 20365
[36] Li X, Guo W and Du Y 2024 *Int. J. Bifurc. Chaos* **34** 2430034
[37] Bao B, Chen L, Bao H, Chen M and Xu Q 2024 *Chaos, Solitons Fractals* **181** 114608
[38] Ma X, Li C, Li Y, Bi L and Qi Z 2022 *Eur. Phys. J. Plus* **137** 542
[39] Li R and Ding R 2021 *Int. J. Mod. Phys. B* **35** 2150166
[40] Wang C, Liang J and Deng Q 2024 *Neural Netw.* **178** 106408
[41] Zhang S, Wang C, Zhang H and Lin H 2024 *Chaos, Solitons Fractals* **186** 115191
[42] Peng Y, He S and Sun K 2021 *AEU Int. J. Electron. Commun.* **129** 153539
[43] Mou J, Han Z, Cao Y and Banerjee S 2024 *IEEE Trans. Circuits Syst.–II: Express Briefs* **71** 2824
[44] He S, Hu K, Wang M, Wang H and Wu X 2024 *Chaos, Solitons Fractals* **188** 115517
[45] Bao H, Hua Z, Li H, Chen M and Bao B 2021 *IEEE Trans. Circuits Syst.: Regul. Pap.* **68** 4534
[46] Ren L, Mou J, Banerjee S and Zhang Y 2023 *Chaos, Solitons Fractals* **167** 113024
[47] Liu X, Mou J, Zhang Y and Cao Y 2024 *IEEE Trans. Ind. Electron.* **71** 5094
[48] Bao B, Hu J, Cai J, Zhang X and Bao H 2023 *Nonlinear Dyn.* **111** 3765
[49] Liu B, Peng X and Li C 2024 *AEU Int. J. Electron. Commun.* **178** 155283
[50] Bao B, Hu J, Bao H, Xu Q and Chen M 2024 *Cogn. Neurodynamics* **18** 539
[51] Li C, Yang Y, Yang X and Lu Y 2022 *Eur. Phys. J. Spéc. Top.* **231** 3209
[52] Liang Z, He S, Wang H and Sun K 2022 *Eur. Phys. J. Plus* **137** 309
[53] Wang H, Xin Z, He S and Sun K 2024 *Phys. Scr.* **99** 095218
[54] Zang H, Fu H, Huang L, Lei T and He S 2025 *Chaos: Interdiscip. J. Nonlinear Sci.* **35** 063114
[55] Yang F, Zhou P and Ma J 2024 *Commun. Theor. Phys.* **76** 035004
[56] Yang F, Ren L, Ma J and Zhu Z 2024 *J. Zhejiang Univ. Sci. A* **25** 382
[57] Yang F, Song X and Ma J 2024 *Chin. J. Phys.* **91** 287
[58] Song X, Wang Y and Yang F 2025 *Commun. Theor. Phys.* **77** 085801
[59] Kong S, Li C, He S, Çiçek S and Lai Q A 2021 *Chin. Phys. B* **30** 110502
[60] Li C, Li Y, Yu W, Moroz I and Volos C 2025 *Nonlinear Dyn.* **113** 3857
[61] Huang H, Li C, Cen X, Gao Y and Liu W 2025 *Int. J. Bifurc. Chaos* **35** 2550037
[62] Li C, Yi C, Li Y, Mitro S and Wang Z 2024 *Chaos: Interdiscip. J. Nonlinear Sci.* **34** 031102